愛知工業大学研究報告
第22号B　昭和62年

On The Mode of Shear Failure of Reinforced Concrete Columns

Takakazu OOI

鉄筋コンクリート柱のせん断破壊様式について

大　井　孝　和

Experimental study on the sudden shear failure of reinforced concrete column under compression-shear bending load was carried out. Careful observations for the specimens lead to a classification of shear failure modes and a forecast to sequential process of failure. To approve these considerations, experimental stress analysis and statistical regression analysis were executed to investigate the conditions of stress re-distribution in the sections near failure, and to estimate quantitative effects of the factors infiuencing shear failure of the specimens.

This report was initially published in the Proceedings (Vol. 1) of the International Symposium on Fundamental Theory of Reinforced and Prestressed Concrete at Nanjing Institute of Technology (PRC) in September 1986. The author is grateful for the given occasion to insert the article in this bulletin.

1. Introduction

The study on the failure mechanism of reinforced concrete under shear bending load has a long history, and its importance is still increasing. Many theories and concepts have been proposed, and investigated by following researches, those are, diagonal tension failure theory, shear compression failure theory, theory of bond failure, truss analogy models, block models cut out from shear span of the beam or column, recent FEM models and so forth [1, 2]. However, it would be noted that any single theory could not perfectly explain the complete behavior of reinforced concrete members under various conditions over whole domain of shear failure. For this reason, we may anticipate the action of plural causes, namely, combined or sequential mechanism of failure.

To enter on this consideration, the precise and systematic understanding for the mode of shear failure is essential. As the first step to approach, more than 120 specimens of reinforced concrete column were tested in this study, under antisymmetrical eccentric axial loading, with special reference to the influence of experimental conditions on the failure modes of the specimens.

2. Outline of the Experiment

The method of loading was selected for reasons of its simplicity and clarity of the principle. The principle of loading is shown in Fig. 1. [3, 4, 5]

Axial force N, shear force Q and bending moment M, those which cause along the span of specimen by force P of testing machine, are written respectively as follows.

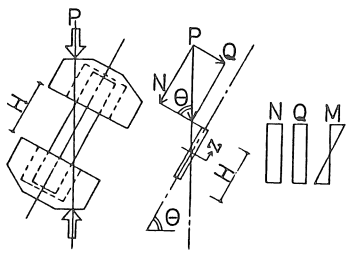

Fig. 1　The principle of loading

$$N = P \cdot \sin\Theta \quad \cdots\cdots\cdots (1)$$
$$Q = P \cdot \cos\Theta \quad \cdots\cdots\cdots (2)$$
$$M = Q \cdot z \quad \cdots\cdots\cdots (3)$$

Where, z : Distance from the center of span, $z = O \rightarrow H/2$, Θ : The inclination of column specimen at loading, whose angle is taken from horizontal line.

Thus, the ratio of axial force N to shear force Q depends upon the angle of inclination of column specimen at loading. The ratio of bending moment M to shear force Q depends upon the span H of the specimen (the value correspond to the story height of structural frames), consequently, this relates to H/D ratio (two times of the shear span ratio), where, D is the depth of column section.

External form of the column specimen is a prism, whose dimensions are, width B=15cm, depth D=15cm (square cross section) and length L is 60cm longer than the loading span H.

Marginal zone of both ends of the specimen has important roles, not only for the anchorage of longitudinal reinforcement but the installation of loading apparatus.

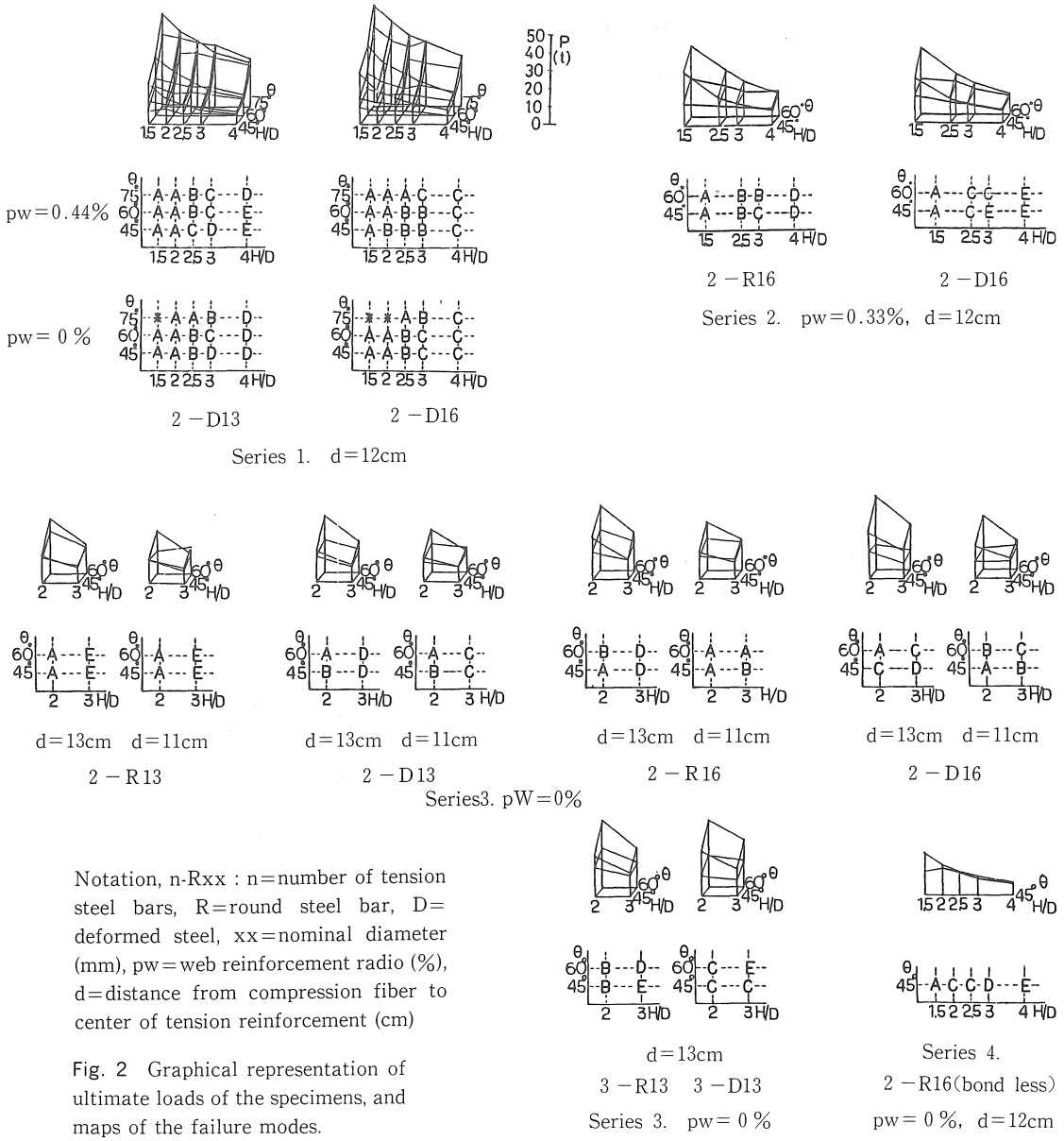

Notation, n-Rxx : n=number of tension steel bars, R=round steel bar, D=deformed steel, xx=nominal diameter (mm), pw=web reinforcement radio (%), d=distance from compression fiber to center of tension reinforcement (cm)

Fig. 2 Graphical representation of ultimate loads of the specimens, and maps of the failure modes.

The loading apparatus consists of rigid steel frames and loading arms made of thick steel plates. Rigid steel frames (stiffener) are attached to the both ends of specimen, 3 or 4 days before testing, and fixed with high strength neat cement paste grouted into narrow space between concrete prism and the frame. The loading arms, provided for loading angle $\Theta=45°$, 60°, 75°, each applicable to the range of $H/D=1.5$ to 4, are attached to the steel frames just before the testing by sets of high tension bolts.

This study includes four series of experiment, each of them have gradually shifting aims and experimental conditions.

Series 1, 60 specimens for the basic deployment of experimental conditions.

Series 2, 20 specimens, the extensive tests for measuring deformation of reinforcing steel.

Series 3, 40 specimens, further development of previous series.

Series 4, 10 specimens for reinforcing steel without bond.

Strength of concrete were fixed for all specimens about 300 kg/cm^2 throughout the series. All speci-

mens, except series 2, were tested under monotonous increasing load.

Items of measurements and observation are, deflection of the specimen by dial gauges, deformation of concrete and reinforcing steel by wire strain gauges, crack initiation and its development of concrete by flexure, the same article by shear force, crack propagation along longitudinal reinforcement, ultimate load and the mode of failure.

Details of raw data have to be omitted here for want of space.

Experimental results of ultimate load were compared with elastic-plastic theory of flexure. As it is well known, in the mode of bending failure, the ratio of experimental to theoretical value is close to 1.0 in usual, while in the mode of shear failure, this ratio becomes lower than 1.0, varying widely with their experimental conditions. This comparison are shown graphically in Fig. 2, with illustrative maps of the failure modes.

The failure modes were classified into five grades from A to E.

Type A : Flexural cracking arises first at both extremes of the span, but the crack growth remains small in scale in the shear tension zone. When diagonal split through the span suddenly occurs, stress is redistributed and load reaches to the ultimate. (Diagonal split — shear compression failure)

Type B : Flexural cracks arise first. Shear tension crack by diagonal tension and longitudinal cracks by bond slip of reinforcement follows to it in small scale. The diagonal splitting crack is distinct and fatal. The split line is sometimes curved or branched off. (Bond slip - diagonal split — shear compression failure)

Type C : Flexural cracks which taken place secondly or later, develop to the inclined shear tension cracks, and quicken the longitudinal cracks along reinforcement. Collapse of compression concrete precedes to diagonal splitting crack in the ultimate. (Bond slip — shear compression failure)

Type D : Process of cracking in flexure and shear tension is similar to type C. Longitudinal cracks along the reinforcement propagate like a row of small shear tension cracks in side faces of specimen, and/or a straight line in bottom face accompanied with transverse openings of flexural cracks. Extension of these cracks leads to the ultimate load. Diagonal splitting crack does not occur. (Bond slip — bending failure)

Type E : Typical mode of bending failure. Bond slip cracks are not found. The ultimate state come to pass after yielding of tension steel and failure of concrete in compression. (Bending failure)

It should be noted that failure of concrete in compression zone is commonly the final cause of the ultimate state for all types of failure written above.

According to Fig. 2, locations of these failure modes on the maps lay always in this order.

As for the ratio of experimental to theoretical values of ultimate load, the averages obtained in this study are, 0.62 for type A, 0.75 for type B, 0.82 for type C, 0.90 for type D, and 0.97 for type E.

The location and territory of the failure modes on the maps are determined mainly by the H/D ratio of the specimen, and the influences of other factors on it are relatively small. On the other hand, the value of experimental to theoretical ratio of ultimate load is influenced largely by the conditions of specimen and loading, for example, H/D ratio, loading angle Θ, the quantity of web reinforcement, and the shapes, sectional areas and placings of the longitudinal reinforcement.

3. Bond Stress Development along Reinforcing Steel

Observed deformation of the specimens were compared strictly with calculated values of flexural theory mentioned above, since it is supposed that the load when experimental data begin to deviate from the predicted behavior of bending is the initiation of shear failure process.

Many facts concerning to the shear failure process were detected in this analysis, i.e. cracking limit

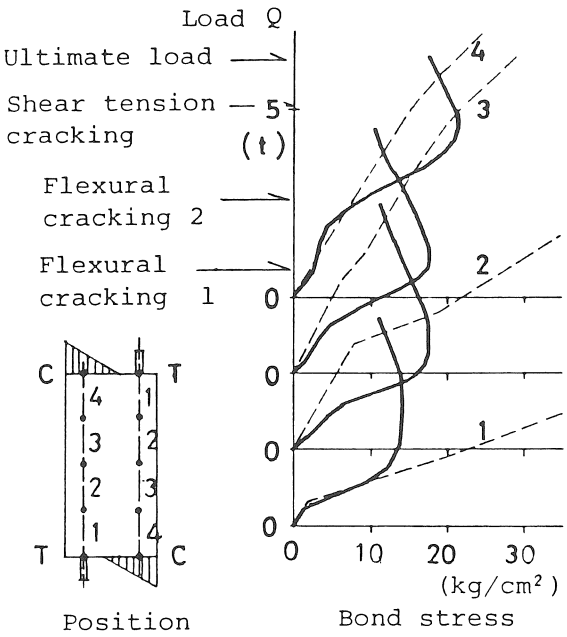

Fig. 3 An example of bond stress dintribution, spcimen Series 3, 2—R16, H/D=3, θ=45°, type D mode.

of concrete stress in shear, influence of web reinforcement on it, longitudinal stress distributions of reinforcing steel, and their behaviours under repeated load. Among them, the result on the bond stress development along reinforcing steel is presented here briefly.

Fig. 3 shows an example of bond stress distribution developed by load Q (shear force component) at several positions of reinforcing steel. In this figure, theoretically predicted bond stresses are indicated by dotted lines, and the experimental values derived from stress of steel bars are indicated by continuous lines.

Following facts can be read out from the figure.

Bond stress around tension steel at the extreme of the span leaves from the tendency of theoretical prediction immediately after the first flexural cracking arise, and turn to increase rapidly.

When the bond stress reaches to a certain value (20～60 kg/cm² for deformed steel, 15～20 kg/cm² for round steell bars), increase of bond stress stops notwithstanding the increase of load, and at the same time, bond stress at the neighboring region turns to a rapid increase.

The stoppage of bond stress increase means a limitation for stress transmission between reinforcing steel and concrete. This results a considerable increase of tension stress in reinforcing steel, so much that compression steel disguise into tension reinforcement, and consequently, the development of bond slip cracking, collapse of concrete in compression, and the fatal diagonal split cracking of the specimen.

4. Statistical Analysis of the Cracking and Ultimate Loads

Statistical analysis is a different possible way to approach this problem. Multiple regression analysis was carried out to obtain quantitative expressions for the influences of experimental factors on the shear cracking and ultimate shear loads.

The results of analysis are shown below. Factors were chosen from the experimental conditions adopted in this study. Estimated effects of the factors are considered to be harmonious with other preceding studies.

$$Q1=bj\{\alpha\cdot{}_cF_s+0.229\left(\frac{N}{b}\right)+0.047(P_w\cdot{}_wF_t)-0.040(P_t\cdot{}_sF_t)-3.37(RD)\} \quad \cdots\cdots(4)$$

$$Q2=bj\{\alpha\cdot{}_cF_s+0.152\left(\frac{N}{b}\right)+0.299(P_w\cdot{}_wF_t)+0.112(P_t\cdot{}_sF_t)-5.42(RD)\} \quad \cdots\cdots(5)$$

$$Qu=bj\{\alpha\cdot{}_cF_s+0.126\left(\frac{N}{b}\right)+0.444(P_w\cdot{}_wF_t)+0.150(P_t\cdot{}_sF_t)-2.27(RD)\} \quad \cdots\cdots(6)$$

Where, Q1 : Initial cracking load of shear tension (kg), shear force component, in the same manner for Q2 and Qu, Q2 : Diagonal split cracking load (kg), Qu : Ultimate load for shear failure (kg), b : Width of rectangular cross section of the specimen (cm), j : Distance from center of resultant compressive stress to center of tension reinforcement (cm), ${}_cF_s$: Shear strength of concrete (kg/cm²), substituted here by tensile strength of concrete obtained from split cylinder test, N/bD : Normalized axial force (kg/cm²), D : Full depth of the cross section (cm), $P_w\cdot{}_wF_t$: Quantity of web reinforcement (kg/cm²), $P_t\cdot{}_sF_t$: Quantity of longitudinal reinforcement (kg/cm²), RD : Round steel bar=0 or deformed steel=1, α : Coefficient affected by shear span ratio M/Qd, definition after the design standard for reinforced concrete structures by the Architectural Institute of Japan (AIJ).

According to the AIJ design standard, Allowable shear resistance Qa for beam is given in the following form, which is the original form for the columns. [6]

$$Qa=bj\{\alpha\cdot{}_cf_s+0.5{}_wf_t(P_w-0.002)\} \quad \cdots\cdots(7)$$

Where, $\alpha=\dfrac{4}{\dfrac{M}{Qd}+1}$ $\cdots\cdots(8)$ and $1\leqq\alpha\leqq2$

Rewrite the expression (8) in a general form, we obtain

$$\alpha=\frac{C2}{\dfrac{M}{QD}+C1}\ ,\quad \text{hence}\quad \alpha\cdot\frac{M}{QD}=-C1\cdot\alpha+C2 \quad \cdots\cdots(9)$$

This relation (8) (9) is expressed as a linear line in a diagram with coordinate axis α and $\alpha(M/QD)$. Graphical representation of eq. (8) is shown in Fig. 4.

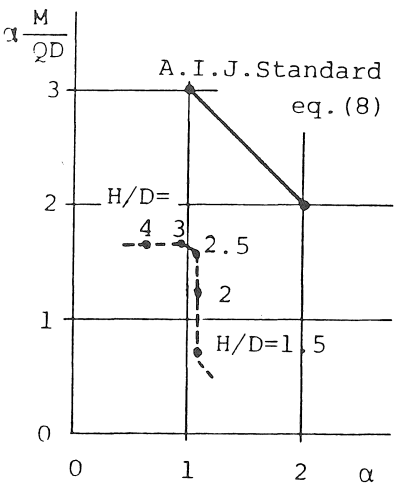

Fig. 4 Characteristics of estimated coefficient α in eq.(5)

Estimation of coefficient α was excluded in the former steps of analysis. Experimental data were corrected by using former results of the analysis, reversely to diminish the variations of the data due to other experimental conditions, and finally we obtained the estimates of coefficient α for eqs. (4) to (6).

The characteristics of the estimated values of coefficient α may be summarized as it is illustrated simultaneously in Fig. 4. This graphical representation suggests that the whole range of the estimated value is to be divided into two parts (trends). The one is a vertical line and the other horizontal line.

In the former trend, where H/D ratio ranges from 1.5 to 2.5, coefficient α is almost a constant, stays nearly about 1.0 or 1.1. While the latter trend, where H/D ratio ranges from 2.5 to 4 in this experiment, coefficient α can be expressed as, $C1=0$, and then $\alpha = C2/(M/QD)$.

It may be allowed to consider these trends of coefficient α, with the first term of right side of the eqs. (4) to (6), which has the major effect for shear failure of the specimens. When this approximation is applied to eqs. (4) to (6), the former trend is expressed as follows,

$$Q=(1.0\sim1.1)bj\cdot{}_cF_s \cdots\cdots(10)$$

or $$\frac{Q}{bj}=(1.0\sim1.1)\cdot{}_cF_s \cdots\cdots(11)$$

Eqs. (10) and (11) indicate that failure of the specimen which belong to the former trend is determined primarily by the shear strength of concrete.

While, the latter trend is expressed as follows,

$$Q=bj\frac{C2}{\left(\frac{M}{QD}\right)}\cdot{}_cF_s \cdots\cdots(12),$$

hence $$M=bDj\cdot C2\cdot{}_cF_s\simeq(C'bd\cdot{}_cF_c)\cdot j \cdots\cdots(13)$$

Where, ${}_cF_c$: Compressive strength of concrete, $(C'bd\cdot{}_cF_c)$ has the same meaning of the resultant compressive force of concrete in the cross sections of the specimens.

Accordingly, eq. (13) suggests that the failure of the specimen which belong to the latter trend is determined by a certain quantity which concerns to the bending failure.

As for the classification of the failure modes proposed in this study, approximately speaking, type A and B belong to the former trend, type D and E belong to the latter, and type C mode locates at the point of intersection of both trends.

5. Conclusions

Intending systematic approach to the complicated phenomena of shear failure of reinforced concrete, an experimental study with column specimens and widely ranged experimental conditions were carried out. The essentials of the considerations are as follows.

(1) Carefully observed failure process of the specimens are classified into five typical modes from type A to type E. Correspondence of the failure modes to the experimental conditions are shown in the maps of Fig. 2.

(2) Bond slip cracking along longitudinal reinforcement plays an important role on the failure process of type B, C and D modes. This sequential mechanism of failure was followed up with experimental stress analysis on concrete and reinforcing steel.

(3) Some quantitative estimations of the experimental factors on the shear cracking and ultimate loads were obtained by a statistical regression analysis. Considerations on the characteristics of estimated coefficient α suggested simply two divisions of the failure modes.

Acknowledgment

This paper is based on research carried out for a decade at the Aichi Institute of Technology. The author greatly appreciate the contributtions of graduate students who joined to the research as their graduation theses.

References

1. Arakawa T. and Takeda H.: On the Shear Reinforcement in Reinforced Concrete Structures (in Japanese), Concrete Journal Vol.17, No.6, June 1976.
2. Shan Bing-Zi : Fundamental Study on the Mechanics of Reinforced Concrete (in Chinese), Printed notes for special lecture held at the Aichi Institute of Technology, Japan, Nov. 1982.
3. Ooi T. : Shear Bending Test on RC Columns by Eccentric Axial Loading (in Japanese), 2627, Summaries of technical papers of the annual meeting AIJ, 1980.
4. Ooi T. : An Experimental Data Analysis for the Shear Resistance of RC Columns (in Japanese), 2360, Summaries of technical papers of the annual meeting AIJ, 1982.
5. Okushima N. and Ooi T. : Influence of the Cover of Concrete for Reinforcement on the Shear Failure of RC Columns (in Japanese), 2797, Summaries of technical papers of the annual meeting AIJ, 1985.
6. Architectural Institute of Japan (AIJ): Design Standard for Reinforced Concrete Structures (in Japanese), § 4. 17, Tokyo, 1982.

(Received January 25. 1987)